NANO LETTERS

2007
Vol. 7, No. 10
3196−3199

# Strength Weakening by Nanocrystals in Ceramic Materials

**Yuejian Wang,* Jianzhong Zhang, and Yusheng Zhao***

*LANSCE-LC, Los Alamos National Laboratory, Los Alamos, New Mexico 87545*

*Received July 31, 2007; Revised Manuscript Received September 4, 2007*

**ABSTRACT**

**A key question in nanomechanics concerns the grain size effects on materials' strength. Correct solution to this question is critical to design and tailor the properties of materials for particular applications. The full map of grain sizes-hardness/yield stress relationship in metals has been built. However, for ceramic materials, the similar studies and understandings are really lacking. Here we employed a novel technique to comparatively study the mechanical features of titanium dioxide ($TiO_2$) with different crystallite sizes. On the basis of peak profile analysis of the X-ray diffraction data, we determined yield strength for nanocrystalline and bulk $TiO_2$. Our results reveal a remarkable reduction in yield strength as the grain size decreases from 30–40 $\mu$m to ~10 nm, providing the only evidence of a strength weakening by nanocrystals relative to their bulk counterparts. This finding infers an inverse Hall–Petch effect, the first of its kind for ceramic materials, and a dramatic strength weakening after the breakdown of classic Hall–Petch relation below a characteristic grain size.**

The classic Hall−Petch relation[1,2] predicts that the strength of a polycrystalline material increases with decreasing grain size. Although this relation is empirically established, it holds well in many crystalline metals and alloys with grain sizes ranging from tens of nanometers to micrometers.[3−5] The Hall−Petch effect is generally attributed to the piling up of dislocations against the grain boundaries, which eventually retards the plastic deformation.[1,2,6] Therefore, in materials of smaller grain size, the increase in the grain boundary concentration would lead to a greater hindrance to the dislocation mobility, and in macroscopic manifestation, an enhanced strength or hardness. The Hall−Petch relation, however, fails in some metals and alloys with grain sizes in the range of 3−20 nm, as demonstrated both experimentally[7−13] and through molecule dynamics simulation.[14−17] In such materials, the strength increased with increased grain size, a phenomenon that is usually referred as an *inverse* Hall−Petch effect. Even though a number of mechanisms have been proposed to explain this effect (see later discussion), it is shown[18] that in several instances, the observed inverse Hall−Petch effect could be the artifacts of conventional indentation measurements, primarily due to the presence of porosity and/or amorphous inclusions in nanocrystalline materials. Because of the high brittleness and low ductility, the conventional indentation and tensile testing methods are both not suitable to study the size effect on ceramic materials and that is the reason why the error-free results concerning ceramics in this topic are real scarcity.

The peak-width analysis of diffraction data for materials' strain/strength is a classic approach widely used in the scientific community, commonly referred as the Williamson−Hall method or its variation.[19−22] This method will overcome the sample porosity or impurity problems commonly faced in the traditional indentation or deformation experiments. Generally speaking, the polycrystalline diffraction profile is a convolution function of instrument response, grain size distribution, and crystal lattice deformations along the diffraction vector. During high-pressure compression experiment, the breaths of diffraction peaks broaden and the amount of peak broadening indicates the distribution of differential strains along the diffraction vector,[23] which is typically owing to different crystalline orientations relative to the loading direction and particularly to the stress concentration at grain-to-grain contacts during the powder compaction. The diffraction peak widths reach the maximum as the deviatoric stress approaches the ultimate yield strength and the sample material begins to flow plastically. By monitoring the peak width variation of different *hkl* diffractions as a function of pressure, one can derive the differential strain, thus the yield strength of the sample materials. In the present study, we conducted in situ synchrotron X-ray diffraction experiment under high pressure and temperature conditions on both nanocrystalline and bulk $TiO_2$. The experimental results reveal an unusual reduction in yield strength as grain size decreases from micrometer to nanometer.

The experiment was carried out using a cubic-anvil high-pressure apparatus, which was interfaced with energy-dispersive synchrotron radiation at the beamline X17B2 of National Synchrotron Light Source, Brookhaven National Laboratory. The experimental methods are similar to those described previously.[24−27] The high-purity (>99%) powdered

* Corresponding authors. E-mail: yzhao@lanl.gov (Y.Z.); yuejianw@lanl.gov (Y.W.).

10.1021/nl0718723 CCC: $37.00 
**Published on Web 09/14/2007**

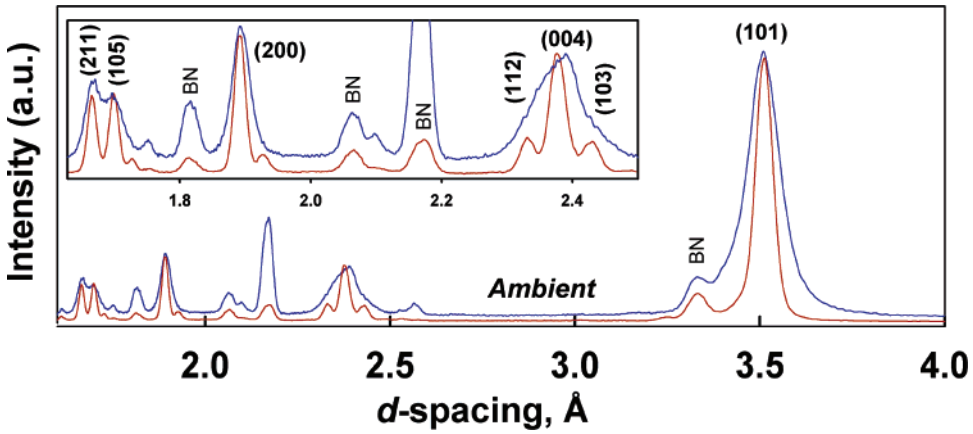


**Figure 1.** X-ray diffraction patterns of nanosized (dark-blue lines) and bulk $TiO_2$-anatase (dark-red lines) at ambient conditions. Inset: Blow-up of the two patterns in the smaller *d*-spacing range. The evident peak broadening of nanosized $TiO_2$ primarily results from the grain size reduction.

nanocrystalline (~10 nm) and bulk (30−40 $\mu$m) $TiO_2$ (anatase) were commercially obtained from Sigma-Aldrich and were studied simultaneously in a single high-pressure experiment. The two samples were loaded in a boron nitride sleeve, separated by a layer of NaCl, which also serves as an internal pressure standard. Such a comparative technique can effectively eliminate the systematic errors of the experiment and allows direct and accurate comparison of materials properties between the sample pair.

Plotted in Figure 1 are the observed X-ray diffraction patterns of nano- and micrometer-$TiO_2$ at ambient conditions. The initial peak broadenings of nano-$TiO_2$ are mainly attributed to the grain size reduction and residual/surface strains.[20] During the experiment, the two samples were compressed to 8.5 GPa by steps of 0.3−0.5 GPa. Figure 2 (top) displays the diffraction peak (101) for nano- and micrometer-$TiO_2$ at selected pressure conditions. It shows that the peaks of both samples become broadened with increasing pressure. However, the rates of peak broadening are quite different for nano- and micrometer-$TiO_2$, which are illustrated in the bottom panel of Figure 2. At 8.5 GPa, the highest pressure of the experiment, micrometer-$TiO_2$ shows 3× increase in the fwhm (full width at half-maximum) relative to that at ambient conditions. For comparison, nano-$TiO_2$ displays only 1.5× augmentation under the identical pressure. This simple comparison indicates that micrometer-$TiO_2$ can support a much higher level of deviatoric stress than its nanocrystalline counterpart.

Following our previous work,[4,28] we express the fwhm of diffraction peaks in a length scale of Å, $\Delta d$(fwhm), which can be used to quantify differential strain ($\epsilon$) introduced by stress heterogeneity, lattice deformation, and dislocation density at high $P-T$. They can also be used to quantify the contributions of instrument response ($\Delta d_{ins}$) and grain sizes ($\Delta d_{size}$),[4,28] in the form of

$$\Delta d_{obs}^2/d^2 = (\epsilon^2 + \Delta d_{ins}^2/d^2) + (\kappa/L)^2 \cdot d^2(P,T) \qquad (1)$$

Here, $\Delta d_{obs}$ and $\Delta d_{ins}$ are the observed peak width and the peak width at a stress-free state, respectively, $d$ is the

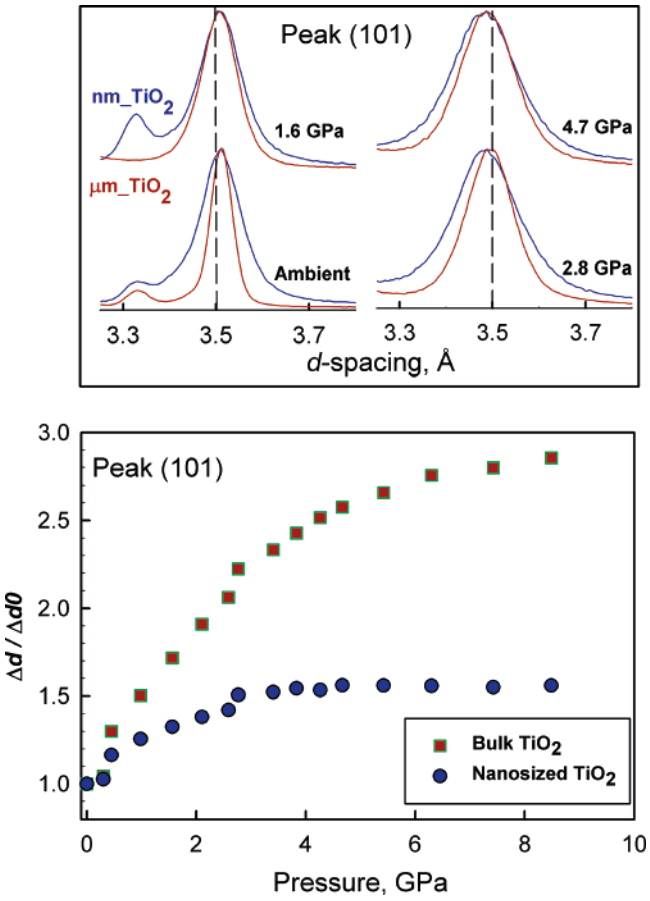


**Figure 2.** Top panel: the (101) diffraction peak of nanosized (dark-blue symbols) and bulk $TiO_2$ (dark-red symbols) at selected pressure conditions. It shows the peak broadening with increasing pressure. Bottom panel: variation of the observed full width at half-maximum, $\Delta d$ (fwhm), for the (101) diffraction line with increasing pressure. The $\Delta d0$ refers to the fwhm at the initial state (i.e., ambient conditions). The figure shows that the rate of peak broadening in bulk $TiO_2$ is significantly higher than that in nano-$TiO_2$. As a result, micrometer-$TiO_2$ can support a much higher level of deviatoric stress than its nanocrystalline counterpart.

*d*-spacing of a given lattice plane, and $L$ the material's grain size, obtained through the incorporation of the Scherrer formula. Note that eq 1 is essentially equivalent to the classic

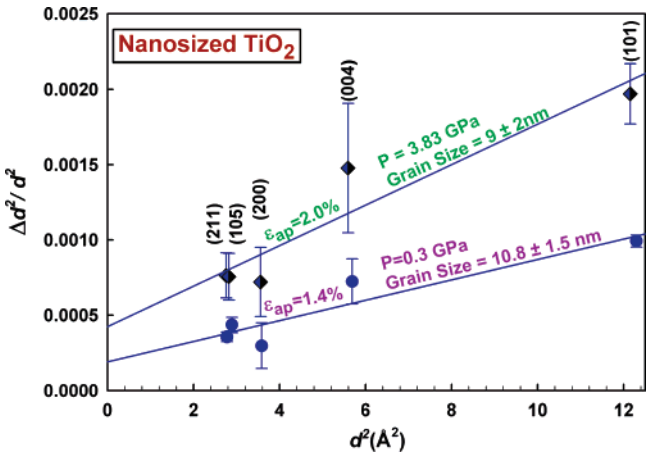


**Figure 3.** Plot of $\Delta d_{obs}^2/d^2$ vs $d^2(P,T)$ according to eq 1 for nano-$TiO_2$ at selected pressures. It illustrates the determination of strain and grain size, respectively, from the intercept and slope of the fitted linear lines.

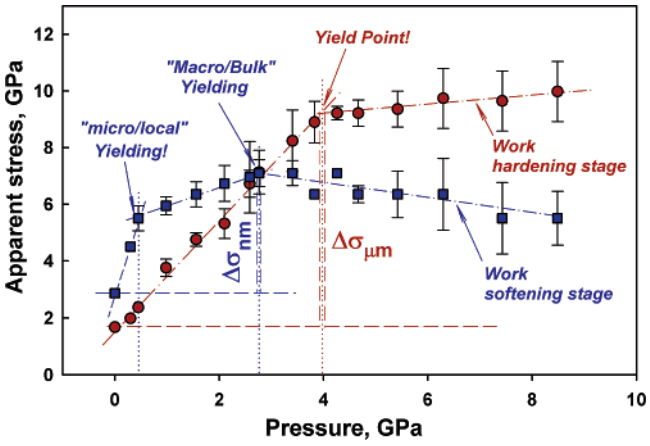


**Figure 4.** Plot of apparent stresses vs pressure for nano-$TiO_2$ (dark-blue solid squares) and bulk $TiO_2$ (dark-red solid circles). A two-stage yielding is clearly revealed for nano-$TiO_2$, one near 0.5 GPa in elastic stage and the other around 2.8 GPa. The first yielding is considered as a "micro/local" yield point,[4,28] representing the local plastic deformation at point-to-point contacts due to high stress concentration. The second yielding point indicates the onset of "macro/bulk" plastic deformation of the entire sample. The enlarged area of stress distribution on grain, from point-to-point contacting in local yielding stage to the entire grain surface, leads to a flatter slope in the macro yielding stage. The onset pressure of yielding in bulk $TiO_2$ is higher and near 4.0 GPa. The apparent stresses plotted in the figure include both strain and instrument broadening; the yield strength can be graphically determined by the difference between the yielding and the initial state, as indicated by $\Delta\sigma_{nm}$ and $\Delta\sigma_{um}$, respectively, for nano- and bulk $TiO_2$.

Williamson−Hall method and its subsequent variations.[4,28] With the fwhm expressed in the length unit of Å, however, eq 1 can be applied to any diffraction data, independent of detecting modes (energy dispersive, angular dispersive, and time-of-flight). Equation 1 is a typical $Y = \boldsymbol{a} + \boldsymbol{b}\cdot X$ plot. Therefore, one can derive the apparent strain $\epsilon^2_{\text{apparent}} = (\epsilon^2 + \Delta d^2_{\text{ins}}/d^2)$ as well as average grain size $L$ from the ordinate intercept and slope of the $\Delta d^2_{obs}/d^2$ versus $d^2(P)$ plot, respectively. Examples of such derivation from diffraction data at 0.3 and 3.83 GPa are illustrated in Figure 3. The apparent strains (also referred as nonuniformed strain) described here are derived from the peak broadening, which are different from the regular strains (uniform strain) expressed as $\Delta V/V$ usually obtained from the peak shift of X-ray diffraction patterns. Such defined apparent strain is determined by the materials strength; the higher the material's strength, the more peak broadening and hence more strains under a given stress level. The detailed description was published somewhere else.[23]

The strains determined from Figure 3 can readily be converted to stresses via the relationship: $\sigma = E\cdot\epsilon$, where $E$ is the Young's modulus and can be calculated from the equation $E = B3(1-2\ \nu)$. For nanosized and bulk $TiO_2$ anatase, the bulk moduli ($B$) are 240 Gpa,[29,30] and 180 Gpa,[31] respectively. With a Poisson's ratio of $\nu = 0.28$ for $TiO_2$,[32] we obtain the Young's modulus values of 316 GPa for nano-$TiO_2$ and 238 GPa for micrometer-$TiO_2$. The calculated apparent stresses (microscopic deviatoric stresses) are plotted as a function of pressure in Figure 4 to elucidate the comparison between nano-$TiO_2$ and micrometer-$TiO_2$. The initial difference observed between nano-$TiO_2$ and micrometer-$TiO_2$ is due to residual stress, surface strain, and grain size effects. As pressure increases, we observe two obvious yield (kink) points for nano-$TiO_2$, one at $P = 0.5$ GPa in the elastic deformation stage and the other at $P = 2.8$ GPa. We consider that the first yield represents "micro/local" grain-to-grain contacts and hence local plastic deformation due to high stress concentration. The second yield represents the onset of "macro/bulk" plastic deformation of the entire sample, and the corresponding stresses are the yield strength. The "macro/bulk" yielding is also well defined for micrometer-$TiO_2$ at a higher pressure of $P = 4.0$ GPa. The two-stage yielding phenomenon, however, is not observed in the micrometer-$TiO_2$, as the data exhibit good linearity in the entire elastic region. In addition, there is an evident work-hardening for the micrometer-$TiO_2$, where the sample can sustain additional 1.0 GPa of differential stress after the yielding when pressure changes from 4.0 to 8.5 GPa. The nano-$TiO_2$, on the other hand, shows a clear work softening after the "macro/bulk" yield.

The yield strength at the corresponding yielding pressures can be graphically determined in Figure 4 by the differences between the yielding and initial states. The derived yield strength is 4.2 ± 1.0 and 7.5 ± 1.5 GPa, respectively, for nano- and micrometer-$TiO_2$. These experimental results indicate a remarkable reduction of yield strength in polycrystalline $TiO_2$ as grain size decreases from 30−40 $\mu$m to ~10 nm, which, to our knowledge, represents the only evidence of a strength weakening by nanocrystals relative to their bulk counterparts. The variation of yield strength of $TiO_2$ with grain size, however, cannot be determined from the present study based on only two distinct grain sizes. Assuming that the classic Hall−Petch relation holds for $TiO_2$ above a certain characteristic length of grain size, $d_c$, our finding infers an inverse Hall−Petch effect for $TiO_2$, the first report of its kind for ceramic materials. Our finding also indicates a dramatic strength weakening after the breakdown of classic Hall−Petch relation below the $d_c$.

In spite of extensive research, the mechanisms leading to the inverse Hall−Petch effect in nanocrystalline materials remains poorly understood. Several models, however, have been proposed, including enhanced Coble creep,[7] invalidation of dislocation pile-ups,[33] dislocation migration through grains,[34] different atomic structures between grain boundary and grain interior phases (core−shell models),[35,36] and grain boundary sliding.[16,17] Other publications suggested that the nanocrystalline material softening was caused by either the deformation in grain boundaries[37,38] or sample preparation methodology.[39] In most of these models, the generation and/or mobility of dislocations in nanocrystalline materials with grain sizes below the $d_c$ are found to be distinct from those involved in materials with larger grain size. Clearly, there is a transition of deformation mechanisms from intragranular to intergranular when grain size is below the $d_c$. Recently, Louchet et al.[40] revisited Hall−Petch law in terms of the collective motion of interacting dislocation, and they attributed the Hall−Petch law breakdown for nanometric-sized grains to the loss of collective effects of dislocation avalanches; instead, the grains are deformed by successive motion of individual dislocations. All these theories, however, are formulated to interpret the observations for metals and alloys. Whether these interpretations are applicable to more brittle and stronger ceramic materials have to date not been explored. Further understanding of our observations for $TiO_2$, both experimentally and theoretically, is expected to provide new insight into nanomechanics and possibly open new opportunities for tailoring the materials' properties.

**Acknowledgment.** This research is supported by the Los Alamos National Laboratory, which is operated by Los Alamos National Security LLC under DOE contract DE-AC52-06NA25396. The experimental work was carried out at the beamline X17B2 of National Synchrotron Light Source, Brookhaven National Laboratory, which is supported by the Consortium for Materials Properties Research in Earth Sciences (COMPRES) under NSF cooperative agreement EAR 01-35554.

## References

(1) Hall, E. O. *Proc. Phys. Soc. London, B* **1951**, *64*, 747.
(2) Petch, N. J. *J. Iron Steel Inst.* **1953**, *174*, 25.
(3) Chen, J.; Schmidt, N.; Chen, J.; Wang, L.; Weidner, J. D.; Zhang, J.; Wang, Y. *J. Mater. Sci.* **2005**, *40*, 5763.
(4) Zhao, Y.; Zhang, J.; Clausen, B.; Shen, T. D.; Gray, G. T., III; Wang, L. *Nano Lett.* **2007**, *7*, 426.
(5) Qian, J.; Pantea, C.; Zhang, J.; Daemen, L. L.; Zhao, Y.; Tang, M.; Uchida, T.; Wang, Y. *J. Am. Ceram. Soc.* **2005**, *88*, 903.
(6) Smith, E. *J. Appl. Phys.* **1970**, *41*, 2736.
(7) Chokshi, A. H.; Rosen, A.; Karch, J.; Gleiter, H. *Scr. Metall.* **1989**, *23*, 1679.
(8) Alves, H.; Ferreira, M.; Köster, U.; Müller, B. *Mater. Sci. Forum* **1996**, *769*, 225.
(9) Lu, K.; Wei, W. D.; Wang, J. T. *Scr. Metall. Mater.* **1990**, *24*, 2319.
(10) Palumbo, G.; Erb, U.; Aust, K. T. *Scr. Metall. Mater.* **1990**, *24*, 2347.
(11) Cheung, H.; Altstetter, C. J.; Averback, R. S. *J. Mater. Res.* **1992**, *7*, 2962.
(12) Khan, A. S.; Zhang, H.; Takacs, L. *Int. J. Plast.* **2000**, *16*, 1459.
(13) Erb, U. *Nanostruct. Mater.* **1995**, *6*, 533.
(14) Swygenhoven, H. V.; Caro, A. *Phys. Rev. B* **1998**, *58*, 11246.
(15) Swygenhoven, H. V.; Spaczer, M.; Caro, A. *Acta Mater.* **1999**, *47*, 3117.
(16) Schiøtz, J.; Tolla, F. D. D.; Jacobsen, K. W. *Nature* **1998**, *391*, 561.
(17) Schiøtz, J.; Vegge, T.; Tolla, F. D. D.; Jacobsen, K. W. *Phys. Rev. B* **1999**, *60*, 11971.
(18) Koch, C. C.; Narayan, J. *MRS Proc.* **2001**, *634*, B5.1.1.
(19) Williamson, G. K.; Hall, W. H. *Acta Metall.* **1953**, *1*, 22.
(20) Klug, H. P.; Alexander, L. E. In *X-ray Diffraction Procedures for Polycrystalline and Amorphous Materials*, 2nd ed.; Klug, H. P., Alexander, L. E., Eds.; John Wiley & Sons: New York, 1974.
(21) Gerward, L.; Morup, S.; Topsoe, H. *J. Appl. Phys.* **1976**, *47*, 822.
(22) Warren, B. In *Series X-ray Diffraction*; Addison-Wesley: London, 1989.
(23) Weidner, D. J.; Wang, Y.; Vaughan, M. T. *Geophys. Res. Lett.* **1994**, *21*, 753.
(24) Weidner, D. J.; Vaughan, M. T.; Ko, J.; Wang, Y.; Liu, X.; Yeganeh-haeri, A.; Pacalo, R. E.; Zhao, Y. In *High-Pressure Research: Application to Earth and Planetary Sciences*; Syono, Y., Manghnani, M. H., Eds.; AGU: Washington DC, 1992; Vol. 67, p 13.
(25) Hazen, R. M. *Science* **1993**, *259*, 206.
(26) Zhang, J.; Li, B.; Utsumi, W.; Liebermann, R. C. *Phys. Chem. Mineral.* **1996**, *23*, 1.
(27) Zhang, J.; Kostak, P. *Phys. Earth Planet. Inter.* **2002**, *129*, 301.
(28) Zhao Y.; Zhang, J. Micro-strain/grain-size analyses from diffraction peak-width and graphic derivation of high $P-T$ thermomechanics. *Int. J. Plast.* **2007**, submitted for publication.
(29) Swamy, V.; Dubrovinsky, L. S.; Dubrovinskaia, N. A.; Simionovici, A. S.; Drakopoulos, M.; Dmitriev, V.; Weber, H. P. *Solid State Commun.* **2003**, *125*, 111.
(30) Pischedda, V.; Hearne, G. R.; Dawe, A. M.; Lowther, J. E. *Phys. Rev. Lett.* **2006**, *96*, 035509.
(31) Arlt, T.; Bermejo, M.; Blanco, M. A.; Gerward, L.; Jiang, J. Z.; Olsen, J. S.; Recio, J. M. *Phys. Rev. B* **2000**, *61*, 14414.
(32) Shackelford, J. F.; Alexander, W. *CRC Materials Science and Engineering Handbook*, 3rd ed.; CRC Press: Boca Raton, FL, 2001; p 766.
(33) Nieman, G. W.; Weertman, J. R.; Siege, R. W. *J. Mater. Res.* **1991**, *6*, 1012.
(34) Lian, J.; Baudelet, B.; Nazarov, A. A. *Mater. Sci. Eng., A* **1993**, *172*, 23.
(35) Gryaznov, V. G.; Gutkin, M. Yu.; Romanov, A. E.; Trusov, L. I. *J. Mater. Sci.* **1993**, *28*, 4359.
(36) Takeuchi, S. *Scr. Mater.* **2001**, *44*, 1483.
(37) Hahn, H.; Padmanabhan, K. A. *Philos. Mag. B* **1997**, *76*, 559.
(38) Hahn, H.; Mondal, P.; Padmanabhan, K. A. *Nanostruct. Mater.* **1997**, *9*, 603.
(39) Sergueeva, A. V.; Stolyarov, V.; Valiev, R. Z.; Mukherjee, A. K. *Scr. Mater.* **2001**, *45*, 747.
(40) Louchet, F.; Weiss, J.; Richeton, T. *Phys. Rev. Lett.* **2006**, *97*, 075504.

NL0718723